J. of Electromagn. Waves and Appl., Vol. 21, No. 14, 1905–1914, 2007

FDTD STUDY ON SCATTERING OF METALLIC COLUMN COVERED BY DOUBLE-NEGATIVE METAMATERIAL

M. Y. Wang and J. Xu

School of Physical Electronics
University of Electronic Science and Technology of China
Chengdu, Sichuan 610054, China

J. Wu, Y. B. Yan, and H. L. Li

China Research Institute of Radiowave Propagation
Beijing 102206, China

Abstract—Electromagnetic scattering of metallic column covered by double-negative (DNG) metamaterials is simulated with auxiliary differential equation method in Finite-Difference Time-Domain method. Lossy Drude polarization and magnetization models are used to simulate DNG media. Numerical result shows that though the backward scattering of metallic column covered by DNG media decrease, the forward scattering increase. The effects to the backward scattering caused by the variation of DNG media's depth, plasma frequency, damping frequency and incident wave frequency are discussed.

1. INTRODUCTION

In 1968 Veselago [1] theoretically stated that media with negative permittivity and permeability would have distinct electromagnetic characteristic. Such as, negative refraction, reversed Doppler shift and reversed Cerenkov radiation. In 2001, inspired by the work of Pendry [2] et al., Smith [3] et al. foremost constructed a composite "medium" in the microwave regime by arranging periodic arrays of small metallic wires and split-ring resonators (SRRs). These kinds of media can also be mentioned metamaterials, negative-index materials, left-handed medium or double-negative (DNG) metamaterials et al.

Many experimental and theoretical investigations [1–15] have been made to study wave propagation property [4–8] and scattering [9–14] of DNG media with different methods and its applications in a highly resolution perfect lens, sub-wavelength compact cavity resonator, enhanced electrically antennas and stealth effect et al. Most of the references, which compute scattering of DNG media, do not consider the effects caused by dispersive characteristic of DNG media.

The differential-equation (DE) method, the integral-equation (IE) method, and the equivalent-circuit models are fundamental numerical methods for characterizing DNG media. Among these methods, the Finite-Difference Time-Domain method (FDTD) is a popular algorithm to predict the properties of DNG media in arbitrary shapes. FDTD can study not only DNG media made of SRRs and metallic wires [15], but also DNG media is equivalent to dispersive media. For the latter case, lossy Drude polarization and magnetization models are often used to simulate DNG media with auxiliary differential equation method in FDTD. Auxiliary differential equation (ADE) method [7, 8], recursive convolution method [16, 17], z-transform method and shift operator method [14] are popularly used to simulate dispersive media. The ADE method has higher precision than the others. The computational cost and memory requirement of ADE method are lower than those of shift operator method.

In the paper, we firstly derive auxiliary differential equation method in FDTD. Then, after the numerical verification of the program being shown, the bistatic and backward radar cross scattering (RCS) of DNG media are computed with ADE method in FDTD. The effects to the backward scattering caused by DNG media's depth, plasma frequency, damping frequency and incident wave frequency are discussed in detail.

2. 2D-FDTD SIMULATOR

Lossy Drude polarization and magnetization models are used to simulate the DNG media [9, 10]. In the frequency domain, this means the permittivity and permeability are described as

$$\begin{aligned} \varepsilon(\omega) &= \varepsilon_0 \left\{1 - \omega_{pe}^2 / \left[\omega(\omega + \mathrm{i}\Gamma_e)\right]\right\} \\ \mu(\omega) &= \mu_0 \left\{1 - \omega_{pm}^2 / \left[\omega(\omega + \mathrm{i}\Gamma_m)\right]\right\} \end{aligned} \tag{1}$$

where ω represents incident wave frequency, ε_0 and μ_0 differently represent vacuum permittivity and permeability. ω_{pe}, ω_{pm}, Γ_e and Γ_m represent electric plasma frequency, magnetic plasma frequency, electric plasma damping frequency and magnetic plasma damping

frequency respectively.

$$\begin{aligned}\mathbf{D} &= \varepsilon\mathbf{E} = \varepsilon_0(1+\chi_e)\mathbf{E} = \varepsilon_0\mathbf{E} + \mathbf{P} = \varepsilon_0\mathbf{E} + \varepsilon_0\chi_e\mathbf{E} \\ \mathbf{B} &= \mu\mathbf{H} = \mu_0(1+\chi_m)\mathbf{H} = \mu_0\mathbf{H} + \mu_0\mathbf{M} = \mu_0\mathbf{H} + \mu_0\chi_m\mathbf{H}\end{aligned} \tag{2}$$

where $\mathbf{D}$, $\mathbf{B}$, $\mathbf{P}$, $\mathbf{M}$, χ_e, χ_m represent electric displacementmagnetic inductionpolarization intensitymagnetizationelectric susceptibility and magnetic susceptibility respectively. By comparing (1) with (2), we obtain

$$\begin{aligned}\mathbf{P} &= -\left\{\varepsilon_0\omega_{pe}^2/\left[\omega(\omega+\mathrm{i}\Gamma_e)\right]\right\}\mathbf{E} \\ \mathbf{M} &= -\left\{\omega_{pm}^2/\left[\omega(\omega+\mathrm{i}\Gamma_m)\right]\right\}\mathbf{H}\end{aligned} \tag{3}$$

Equation (3) can be rewritten as

$$\begin{aligned}\left[-(-\mathrm{i}\omega)^2 - (-\mathrm{i}\omega)\Gamma_e\right]\mathbf{P} &= -\varepsilon_0\omega_{pe}^2\mathbf{E} \\ \left[-(-\mathrm{i}\omega)^2 - (-\mathrm{i}\omega)\Gamma_m\right]\mathbf{M} &= -\omega_{pm}^2\mathbf{H}\end{aligned} \tag{4}$$

By using the transform relation between frequency domain and time domain ($\mathrm{i}\omega \to \partial/\partial t$), we get

$$\begin{aligned}\partial^2\mathbf{P}/\partial t^2 + \Gamma_e\partial\mathbf{P}/\partial t &= \varepsilon_0\omega_{pe}^2\mathbf{E} \\ \partial^2\mathbf{M}_n/\partial t^2 + \Gamma_m\partial\mathbf{M}_n/\partial t &= \mu_0\omega_{pm}^2\mathbf{H}\end{aligned} \tag{5}$$

The normalized magnetization is introduced to make the electric and magnetic field equations completely symmetric, i.e., $\mathbf{M}_n = \mathbf{M}\mu_0$. By introducing the induced electric and magnetic currents

$$\mathbf{J} = \partial\mathbf{P}/\partial t \qquad \mathbf{K} = \partial\mathbf{M}_n/\partial t \tag{6}$$

The time domain equations solved with the FDTD simulator for the matched DNG media are

$$\begin{aligned}\nabla\times\mathbf{H} &= \varepsilon_0\partial\mathbf{E}/\partial t + \mathbf{J} & \nabla\times\mathbf{E} &= -\mu_0\partial\mathbf{H}/\partial t - \mathbf{K} \\ \partial\mathbf{J}/\partial t + \Gamma_e\mathbf{J} &= \varepsilon_0\omega_{pe}^2\mathbf{E} & \partial\mathbf{K}/\partial t + \Gamma_m\mathbf{K} &= \mu_0\omega_{pm}^2\mathbf{H}\end{aligned} \tag{7}$$

where $\mathbf{K}$ has been normalized by μ_0 to make the magnetic current equation dual to the electric current definition.

Equations (7) are discretized with the standard grid, leapfrog in time approach. The electric field and electric current are taken at the cell edge for integer time steps; the magnetic field and magnetic current are taken at the cell center for half-integer time steps. Here we only

give TM case. The discretized E_z and J_z in the 2D-FDTD simulators are

$$E_z^{n+1}(i,j) = E_z^n(i,j) - \frac{\Delta t}{\varepsilon_0} J_z^n(i,j) + \frac{\Delta t}{\varepsilon_0}\left[\frac{H_y^{n+1/2}\left(i+\frac{1}{2},j\right) - H_y^{n+1/2}\left(i-\frac{1}{2},j\right)}{\Delta x} - \frac{H_x^{n+1/2}\left(i,j+\frac{1}{2}\right) - H_x^{n+1/2}\left(i,j-\frac{1}{2}\right)}{\Delta y}\right]$$

$$J_z^{n+1}(i,j) = \frac{1-0.5\Gamma_e\Delta t}{1+0.5\Gamma_e\Delta t} J_z^n(i,j) + \frac{\varepsilon_0\omega_{pe}^2\Delta t}{1+0.5\Gamma_e\Delta t} E_z^{n+1}(i,j) \quad (8)$$

3. RESULTS AND DISCUSSION

3.1. Numerical Verification

To demonstrate the validity of auxiliary differential equation method formulation and program for DNG media, Fig. 1 shows the phase compensation characteristic of DNG media. As shown in Fig. 2, a Continuous Wave (CW) Gaussian beam is launched toward a pair of double-positive (DPS) and DNG layers. The CW frequency is chosen to be $f_0 = 30\,\text{GHz}$. Each layer having a thickness of $2\lambda_0 = 2\,\text{cm}$. The DPS slab has $n(\omega_0) = 3$, while the DNG layer has $n_{\text{real}}(\omega_0) \approx -3$, i.e., Eq. (4), in which $\omega_{pe} = \omega_{pm} = \omega_p = 30\,\text{GHz}$, $\Gamma_e = \Gamma_e = \Gamma = 0.1\,\text{GHz} \ll \omega_{pe}$. The FDTD cell size is $\delta = \lambda_0/50$ and the time step $\Delta t = \delta/2c$. The waist of the beam is $w_0 = 17.5\delta$. The electric field intensity distribution is measured at $t = 7500\Delta t$. The beam expands in the DPS slab and then refocuses in the DNG slab (due to its negative index), and the waist of the intensity of the beam is recovered at the back face. The result agrees with the result of Fig. 2 in reference [7]. Therefore the paper's method and program are accurate.

3.2. Bistatic RCS

Figure 2(a) shows the diagram of metallic column covered by DNG media. The bistatic radar cross section when transverse electric (TE) wave and transverse magnetic (TM) wave irradiate on metallic column covered by DNG media are given in Fig. 2 (b) and (c) respectively. The

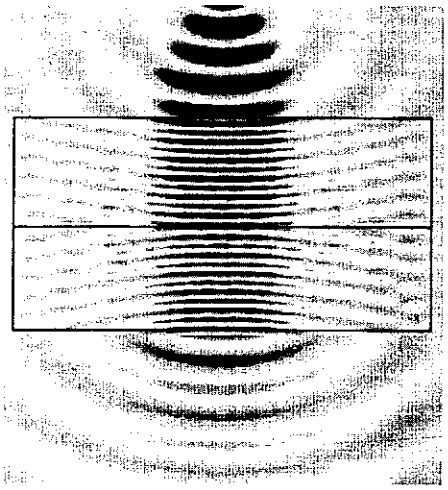

Figure 1. FDTD predict electric-field intensity distribution for the phase compensator system of a DPS-DNG stacked pair.

solid line and the -Δ- represent bistatic RCS of metallic column and metallic column covered by DNG media respectively. The frequency of incident wave is $f_0 = 6\,\mathrm{GHz}$, The FDTD cell size is $\delta = \lambda_0/20 = 0.25\,\mathrm{cm}$ and the time step $\Delta t = \delta/2c$. The radius of metallic column is 0.2 m as shown in Fig. 2(a). The radius of DNG media is 0.025 m, the DNG media has $n(\omega_0) = -6.0361 + 0.0187i$, i.e., Eq. (1), in which $\omega_p = 100\,\mathrm{GHz}$, $\Gamma = 0.1\,\mathrm{GHz} \ll \omega_p$. Though the loss characteristic of DNG media make the RCS decrease of different degree in quite broad angles, the forward scattering (zero degree angle) and the RCS of little bistatic angles (near zero degree angle) increase inversely. Due to the DNG media's possible capability of guiding wave, the energy of incident wave reaches the shadow of column as traveling wave, then the forward scattering increase. The scattering characteristic of DNG media is very similar to that of plasma [17], because they are simulated with lossy Drude polarization and magnetization models.

3.3. Backward Scattering

In Fig. 3, we give the broadband backward radar cross section (have been normalized by wavelength) of metallic column covered by DNG media with different parameters. The radius of the metallic column is 2 cm as shown in Fig. 2(a). The FDTD cell size is $\delta = 0.05\,\mathrm{cm}$, and the time step $\Delta t = \delta/2c$. Fig. 3(a) gives the results with DNG media layer's depth 2 cm. The dash, solid and thick dash lines represent

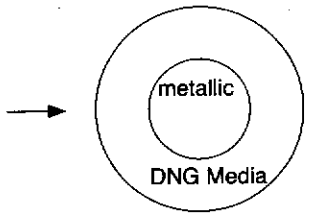

(a)

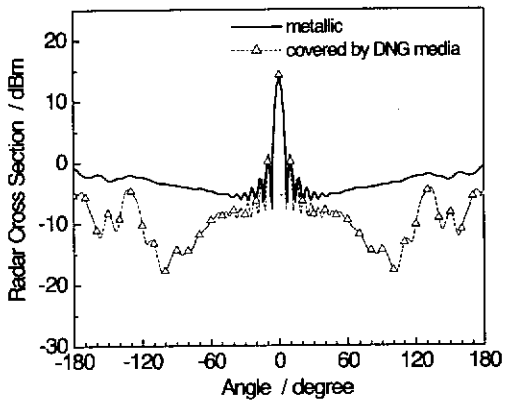

(b)

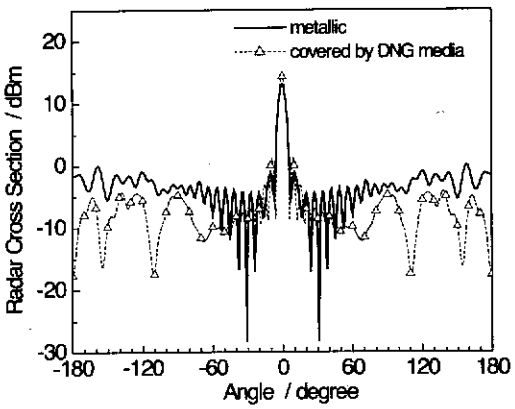

(c)

Figure 2. Metallic column covered by DNG media and bistatic scattering of metallic column covered by DNG media. (a) Metallic column covered by DNG media. (b) TM wave. (c) TE wave.

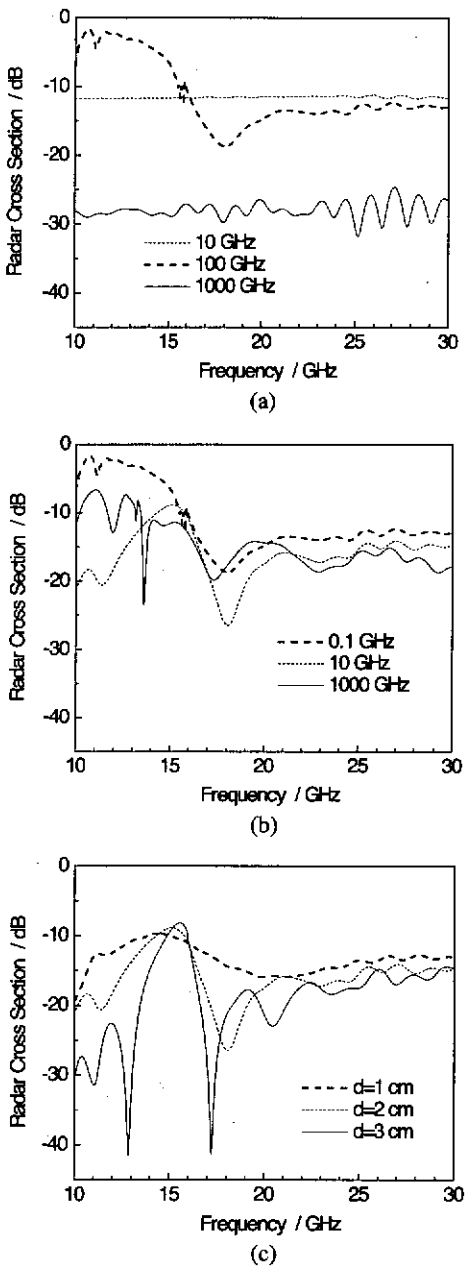

Figure 3. Backward scattering of metallic column covered by DNG media. (a) Plasma frequency varies. (b) Plasma damping frequency varies. (c) Depth varies.

RCS of metallic column without covering layer, DNG media with $\Gamma = 0.1\,\text{GHz}$, $\omega_p = 100\,\text{GHz}$, and $\omega_p = 1000\,\text{GHz}$ respectively. In Fig. 2(b), the depth of the DNG media layer is 2 cm, and $\omega_p = 100\,\text{GHz}$. The dash, solid, and thick dash lines represent $\Gamma = 0.1\,\text{GHz}$, 10 GHz, 1000 GHz respectively. In Fig. 3(c), DNG media's $\omega_p = 100\,\text{GHz}$, $\Gamma = 0.1\,\text{GHz}$, the dash, thick dash and solid lines represent the depth of DNG media $d = 1\,\text{cm}$, 2 cm, 3 cm respectively.

Figure 2(a) shows that DNG media may decrease the target's RCS in quite broad frequency bands. The increase of plasma frequency leads to the decrease of RCS of targets covered by DNG media. In Fig. 2(b), in relatively lower frequencies, the RCS firstly decrease with the increase of DNG media's damping frequency from 0.1 GHz to 10 GHz, and then increase in 1000 GHz. However, in higher frequencies, the RCS decrease with the increase of DNG media damping frequency. Fig. 2(c) shows that the increase of DNG media's depth can reduce its backward scattering in some frequency bands.

4. CONCLUSION

The auxiliary differential equation method in FDTD was derived for DNG media. The bistatic and backward RCS of metallic column covered by DNG media are computed. Numerical result shows that the backward scattering of metallic column covered by DNG media decrease, however the forward scattering increase. The backward scattering of metallic column covered by DNG media is influenced by DNG media's depth, plasma frequency, damping frequency, and incident wave frequency. With a careful selection of DNG media's parameters, the echo of radar targets can be effectively decreased.

ACKNOWLEDGMENT

This work was supported by National Key Laboratory of Electromagnetic Environment fund under Grant No. 51486030305HT0101.

REFERENCES

1. Veselago, V. G., "The electrodynamic of substances with simultaneously negative values of ε and μ," *Sov. Phys. Usp.*, Vol. 10, No. 4, 509–514, 1968.
2. Pendry, J. B., A. J. Holden, D. J. Robbins, and W. J. Stewart, "Magnetism from conductors and enhanced nonlinear phenomena," *IEEE Trans. Microwave Theory Tech.*, Vol. 47, No. 11, 2075–2084, 1999.

3. Shelby, R. A., D. R. Smith, and S. Schultz, "Experimental verification of a negative index of refraction," *Science*, Vol. 292, No. 6, 77–79, 2001.
4. Chen, H., L. Ran, J. Huangfu, X. M. Zhang, K. Chen, T. M. Grzegorczyk, and J. A. Kong, "Negative refraction of a combined double S shaped metamaterial," *Appl. Phys. Lett.*, Vol. 86, No. 15, 151909, 2005.
5. Yao, H. Y., W. Xu, L. W. Li, Q. Wu, and T.-S. Yeo, "Propagation property analysis of metamaterial constructed by conductive SRRs and wires using the MGS-based algorithm," *IEEE Trans. Microwave Theory Tech.* (Special issue on metamaterials), Vol. 53, No. 4, 1469–1476, 2005.
6. Chen, H., B.-I. Wu, and J. A. Kong, "Review of electromagnetic theory in left-handed materials," *J. of Electromagn. Waves and Appl.*, Vol. 20, No. 15, 2137–2151, 2006.
7. Engheta, N. and R. W. Ziolkowski, "A positive future for double-negative metamaterials," *IEEE Trans. Microwave Theory Tech.*, Vol. 53, No. 4, 1535–1556, 2005.
8. Ziolkowski, R. W. and E. Heyman, "Wave propagation in media having negative permittivity and permeability," *Physics Review E*, Vol. 64, 056625, 1–15, 2001.
9. Yao, H. Y., L. W. Li, C. W. Qiu, Q. Wu, and Z. N. Chen, "Scattering properties of electromagnetic waves in a multilayered cylinder filled with double negative and positive materials," *Radio Sci.*, Vol. 42, No. 2, RS2006, 2007.
10. Cheng, D., "Green dyadic and dipole radiation in an electrical-magnetic coupling composite material," *J. of Electromagn. Waves and Appl.*, Vol. 18, No. 3, 381–386, 2004.
11. Li, C. and Z. Shen, "Electromagnetic scattering by a conducting cylinder coated with metamaterials," *Progress In Electromagnetics Research*, PIER 42, 91–105, 2003.
12. Shooshtari, A. and A. R. Sebak, "Electromagnetic scattering by parallel metamaterial cylinders," *Progress In Electromagnetics Research*, PIER 57, 165–177, 2006.
13. Geng, Y. l. and S. l. He, "Analytical solution for electromagnetic scattering from a sphere of uniaxial left-handed material," *Journal of Zhejiang University Science A*, Vol. 17, No. 1, 99–104, 2006.
14. Wang, M. Y., D. B. Ge, J. Xu, and J. Wu, "FDTD study on back scattering of conducting sphere coated with double-negative metamaterials," *International Journal of Infrared and Millimeter Waves*, Vol. 28, No. 2, 199–206, 2007.

15. Semouchkina, E. A., G. B. Semouchkin, M. Lanagan, and C. A. Randall, "FDTD study of resonance processes in metamaterials," *IEEE Trans. Microwave Theory Tech.*, Vol. 53, No. 4, 1477–1487, 2005.
16. Qian, Z. H., R. S. Chen, K. W. Leung, and H. W. Yang, "FDTD analysis of microstrip patch antenna covered by plasma sheath," *Progress In Electromagnetics Research*, PIER 52, 173–183, 2005.
17. Liu, S. B., J. J. Mo, and N. C. Yuan, "FDTD analysis of electromagnetic reflection by conductive plane covered with magnetized inhomogeneous plasmas," *International Journal of Infrared and Millimeter Waves*, Vol. 23, No. 12, 1803–1815, 2002.